

**High-Pressure Chemistry** | *Very Important Paper*
**VIP High-Pressure High-Temperature Synthesis of Mixed Nitridosilicatephosphates and Luminescence of  $AE\text{SiP}_3\text{N}_7:\text{Eu}^{2+}$  ( $AE = \text{Sr}, \text{Ba}$ )**

 Lucien Eisenburger,<sup>[a]</sup> Oliver Oeckler,<sup>\*[b]</sup> and Wolfgang Schnick<sup>\*[a]</sup>
*Dedicated to Professor Thomas M. Klapötke on the occasion of his 60th birthday*

**Abstract:** Tetrahedra-based nitrides with network structures have emerged as versatile materials with a broad spectrum of properties and applications. Both nitridosilicates and nitridophosphates are well-known examples of such nitrides that upon doping with  $\text{Eu}^{2+}$  exhibit intriguing luminescence properties, which makes them attractive for applications. Nitridosilicates and nitridophosphates show manifold structural variability; however, no mixed nitridosilicatephosphates except  $\text{SiPN}_3$  and  $\text{SiP}_2\text{N}_4\text{NH}$  have been described so far. The compounds  $AE\text{SiP}_3\text{N}_7$  ( $AE = \text{Sr}, \text{Ba}$ ) were synthesized by a high-pressure high-temperature approach using the multianvil technique (8 GPa, 1400–1700 °C) starting from the respec-

tive alkaline earth azides and the binary nitrides  $\text{P}_3\text{N}_5$  and  $\text{Si}_3\text{N}_4$ . The latter were activated by  $\text{NH}_4\text{F}$ , probably acting as a mineralizing agent.  $\text{SrSiP}_3\text{N}_7$  and  $\text{BaSiP}_3\text{N}_7$  were obtained as single crystals. They crystallized in the barylite-10 ( $M = \text{Sr}$ ) and barylite-20 structure types ( $M = \text{Ba}$ ), respectively, with P and Si being occupationally disordered. Cation disorder was further supported by solid-state NMR spectroscopy and energy-dispersive X-ray spectroscopy (EDX) mapping of  $\text{BaSiP}_3\text{N}_7$  with atomic resolution. Upon doping with  $\text{Eu}^{2+}$ , both compounds showed blue emission under UV excitation.

## Introduction


Emerging environmental consciousness has pushed the development of solid-state lighting solutions forward. The invention of efficient InGaN-based blue LEDs (light-emitting diodes) enabled the development of pc-LEDs (phosphor-converted) with remarkable properties in terms of color temperature, color rendition, and efficacy. Significant improvements in the aforementioned properties were possible due to nitride compounds such as  $M_2\text{Si}_5\text{N}_8:\text{Eu}^{2+}$  ( $M = \text{Sr}, \text{Ba}$ ),  $M\text{Si}_2\text{O}_2\text{N}_2:\text{Eu}^{2+}$  ( $M = \text{Ca}, \text{Sr}, \text{Ba}$ ),  $\text{SrLiAl}_3\text{N}_4:\text{Eu}^{2+}$ , and  $\text{MAiSiN}_3:\text{Eu}^{2+}$ .<sup>[1–4]</sup>


Materials properties concerning solid-state lighting can be tuned by dopant concentration to a limited extent, affecting Stokes shifts in emission spectra, or by a variation of the size of coordination polyhedra by substitution such as introducing Sr on Ba sites. Completely shifted emission properties, however, can only be achieved by a fundamental alteration of the host lattice.<sup>[5,6]</sup>

The main goal of this work was to expand the compositional and structural diversity of tetrahedra-based luminescent materials. Thus, discovery of the title compounds  $\text{SrSiP}_3\text{N}_7$  and  $\text{BaSiP}_3\text{N}_7$  opens up the novel compound class of mixed nitridosilicatephosphates, which can now be further explored as innovative host lattices. While nitridosilicates have been investigated thoroughly and nitridophosphates show similar promising structures and properties, only two compounds that contain both  $\text{SiN}_x$  ( $x = 4, 6$ ) and  $\text{PN}_4$  units have been reported so far, that is,  $\text{SiPN}_3$  and  $\text{SiP}_2\text{N}_4\text{NH}$ .<sup>[7–9]</sup> The crystal structure of  $\text{SiPN}_3$  corresponds to a defect wurtzite-type arrangement with mixed occupation of Si and P at the tetrahedral sites. The crystal structure of  $\text{SiP}_2\text{N}_4\text{NH}$  is related to sillimanite-type  $\text{Al}_2\text{SiO}_5$ . It is built up from edge-sharing  $\text{SiN}_6$  octahedra interconnected by all-side vertex-sharing  $\text{PN}_4$  tetrahedra. A possible explanation for the challenges concerning syntheses that are involved in the preparation of mixed nitridosilicatephosphates could be the chemical inertness of  $\text{Si}_3\text{N}_4$ , while  $\text{P}_3\text{N}_5$  already decomposes at temperatures above 850 °C if no external pressure is applied. As shown in previous publications, according to Le Chatelier's

[a] L. Eisenburger, Prof. Dr. W. Schnick  
 Department of Chemistry  
 University of Munich  
 Butenandtstraße 5–13, 81377 Munich (Germany)  
 E-mail: wolfgang.schnick@uni-muenchen.de

[b] Prof. Dr. O. Oeckler  
 Institute for Mineralogy, Crystallography and Materials Science  
 Leipzig University  
 Scharnhorststraße 20, 04275 Leipzig (Germany)  
 E-mail: oliver.oeckler@gmx.de

 Supporting information and the ORCID identification numbers for the authors of this article can be found under:  
<https://doi.org/10.1002/chem.202005495>.

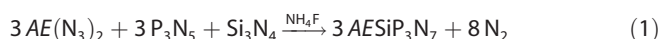
 © 2021 The Authors. *Chemistry - A European Journal* published by Wiley-VCH GmbH. This is an open access article under the terms of the Creative Commons Attribution Non-Commercial NoDerivs License, which permits use and distribution in any medium, provided the original work is properly cited, the use is non-commercial and no modifications or adaptations are made.

principle, the decomposition of  $P_3N_5$  under the formation of  $N_2$  is suppressed by external pressure.<sup>[10]</sup>

$NH_4Cl$  has been successfully employed as a mineralizer facilitating crystal growth of nitridophosphates.  $HCl$  formed in situ most likely leads to reversible P–N bond formation and cleavage.<sup>[11,12]</sup> After nitridosilicatephosphates proved to be not accessible with the help of  $NH_4Cl$ , changing the mineralizing agent to  $NH_4F$  afforded the title compounds  $AE SiP_3N_7$  ( $AE = Sr, Ba$ ). This may be explained by the fact that  $HF$  cannot only reversibly cleave and form P–N bonds, but also Si–N bonds. The surface of  $Si_3N_4$  features  $SiNH_2$  groups that can be attacked by  $F^-$  in a nucleophilic substitution.<sup>[13]</sup>

## Results and Discussion

The nitridosilicatephosphates  $AE SiP_3N_7$  ( $AE = Sr, Ba$ ) were synthesized by high-pressure high-temperature (HP/HT) reactions at 8 GPa and 1400 °C (Ba) and 1700 °C (Sr), respectively, using a modified Walker-type multianvil apparatus.<sup>[14]</sup> The synthesis of  $SrSiP_3N_7$  at temperatures below 1700 °C resulted in samples with significant amounts of unknown side phases. Reactions followed the so-called azide route using  $P_3N_5$ ,  $Si_3N_4$ , and the respective metal azide as starting materials with additional  $NH_4F$  ( $\approx 5$  wt%) as a mineralizing agent [Eq. (1)]. To investigate luminescence properties, samples with the addition of approximately 1 mol% of  $EuF_3$  (concerning  $AE^{2+}$ ) to the starting mixture were prepared.



The title compounds were obtained as colorless powders ( $Eu^{2+}$ -doped samples of  $SrSiP_3N_7$  show a yellow tint) and showed no sensitivity to air or moisture. More detailed information on the HP/HT synthesis is given in the Supporting Information.

The crystal structures were elucidated by single-crystal X-ray diffraction (SCXRD) using direct methods and least-squares refinement.  $SrSiP_3N_7$  crystallizes in space group  $Pmn2_1$  (no. 31) with  $Z=2$ .  $BaSiP_3N_7$  crystallizes in space group  $Pnma$  (no. 62) with  $Z=4$ ; details are given in Tables 1 and S2–7. In addition, Rietveld refinements indicate the presence of  $BaSiP_3N_7$  crystallizing in space group  $Pmn2_1$  (no. 31) with  $Z=2$  as a side phase. Both compounds are isotypic to the two polymorphs of barylite  $BaBeSi_2O_7$ .  $SrSiP_3N_7$  corresponds to the barylite-10 polymorph, whereas  $BaSiP_3N_7$  features the structure of barylite-20. The structures of barylite-10 and barylite-20 represent the maximum degree of order (MDO) polytypes of their polytype family. Both structures consist of a network of all-vertex-sharing  $PN_4$  and  $(Si_{0.5}P_{0.5})N_4$  tetrahedra and elongated square pyramid ( $J_8$ )  $AEN_9$  ( $AE = Sr, Ba$ ) polyhedra (Figure S1).<sup>[15]</sup>

The main difference between the two polymorphs concerns the arrangement of tetrahedra. While in  $SrSiP_3N_7$  all tetrahedra vertices point in the same direction, those in  $BaSiP_3N_7$  alternate, which results in a doubled unit cell with  $2b$  ( $SrSiP_3N_7$ ) =  $a$  ( $BaSiP_3N_7$ ) (Figure 1). Although tetrahedra orientation differs in both compounds, the environment of  $AE$  atoms is strikingly similar. The tetrahedra connection patterns show that both

**Table 1.** Crystallographic data of the single-crystal structure refinements of  $AE SiP_3N_7$  ( $AE = Sr, Ba$ ). Standard deviations are given in parentheses.

Formula	$SrSiP_3N_7$	$BaSiP_3N_7$
molar mass [g mol <sup>-1</sup> ]	306.69	356.41
crystal system	orthorhombic	orthorhombic
space group	$Pmn2_1$ (no. 31)	$Pnma$ (no. 62)
lattice parameters [Å]	$a = 11.979(2)$ $b = 4.9040(10)$ $c = 4.6870(9)$	$a = 9.9048(3)$ $b = 12.1858(3)$ $c = 4.73580(10)$
cell volume [Å <sup>3</sup> ]	275.34(10)	571.60(3)
formula units/unit cell	2	4
density [g cm <sup>-3</sup> ]	3.699	4.142
$\mu$ [mm <sup>-1</sup> ]	10.807	7.927
temperature [K]	296(2)	297(2)
absorption correction	semiempirical	
radiation	Mo-K $\alpha$ ( $\lambda = 0.71073$ Å)	
F(000)	292	656
$\theta$ range [°]	$3.4 \leq \theta \leq 44.09$	$3.34 \leq \theta \leq 38.44$
total no. of reflections	9890	10 523
Independent reflections [ $I \geq 2\sigma(I)$ /all]	1253/1379	959/1128
$R_{\sigma}$ , $R_{int}$	0.0393, 0.0952	0.0234, 0.0481
refined parameters	60	58
goodness of fit	1.100	1.044
R-values [ $I \geq 2\sigma(I)$ ]	$R1 = 0.0293$ $wR2 = 0.0731$	$R1 = 0.0261$ $wR2 = 0.0576$
R-values (all data)	$R1 = 0.0343$ $wR2 = 0.0750$	$R1 = 0.0340$ $wR2 = 0.0599$
$\Delta\rho_{max}$ , $\Delta\rho_{min}$ [e Å <sup>-3</sup> ]	2.18, -1.49	0.81, -1.53

compounds consist of *dreier*, *vierer*, and *sechser* rings that, apart from slight distortions, are arranged and distributed in the same manner (Figure 2), leading to the same topology point symbol  $\{3^2.4^3.5.6^4\}\{3^4.4^5.5^4.6^2\}$ .<sup>[16]</sup> Both compounds exhibit one tetrahedrally coordinated site shared by Si and P, while the other site is solely occupied by P. Further details of the crystal structure investigations may be obtained from the joint CCDC/FIZ Karlsruhe online deposition service by quoting the deposition numbers CSD-2050660 and 2050661. In the case of  $SrSiP_3N_7$ , potential ordering of Si and P was considered by symmetry reduction and refinement of the structure against SCXRD data in the subgroups  $P2_1$ ,  $Pn$ , and  $Pm$  of space group  $Pmn2_1$ . However, no indications of complete ordering were found. In all structure models, the volumes of the resulting four symmetrically independent tetrahedra were compared as (P,Si)–N bond lengths were not sufficiently meaningful for discrimination.<sup>[17]</sup> This investigation led to two different kinds of tetrahedra.

Structure models in subgroups  $P2_1$ ,  $Pn$ , and  $Pm$  reveal two tetrahedra exhibiting a volume of 2.21–2.24 Å<sup>3</sup> that coincides with the volume of  $PN_4$  tetrahedra from known nitridophosphates in literature and corresponds to one site in the final structure model in  $Pmn2_1$ . The other two tetrahedra have a volume of 2.37–2.40 Å<sup>3</sup>, which lies between the volumes of  $PN_4$  (2.13–2.28 Å<sup>3</sup>) and  $SiN_4$  tetrahedra (2.52–2.76 Å<sup>3</sup>) (Tables S10 and 11).<sup>[8,9,26–28,18–25]</sup> BVS (bond valence sum) calculations performed on all structure models revealed two tetrahedral sites fully occupied by P and two tetrahedral sites occupied by Si and P in a 1:1 ratio (Tables S13–15).<sup>[29]</sup>

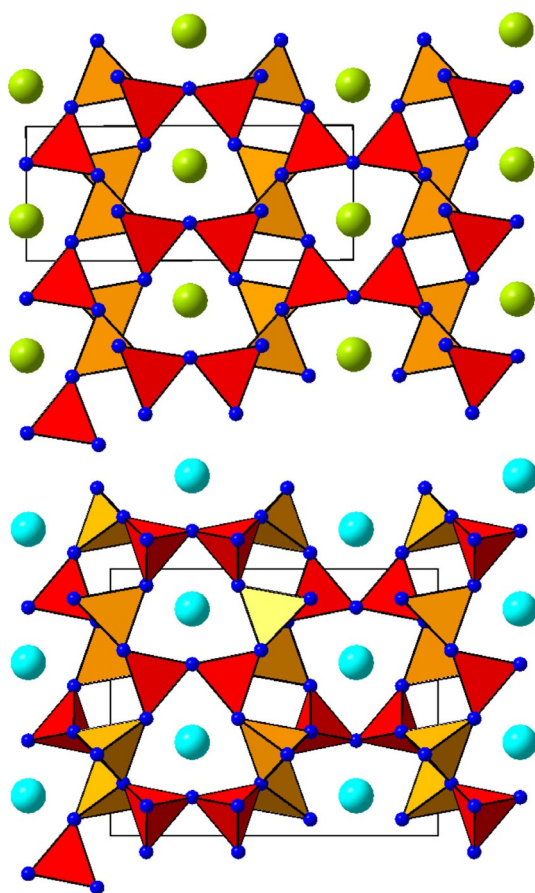


**Figure 1.** Crystal structures of  $\text{SrSiP}_3\text{N}_7$  (top) and  $\text{BaSiP}_3\text{N}_7$  (bottom) both along  $[001]$ . For  $\text{SrSiP}_3\text{N}_7$   $\text{PN}_4$  tetrahedra (red) and  $(\text{Si}_{0.5}\text{P}_{0.5})\text{N}_4$  (orange) all vertices point in the same direction (behind the plane of projection). For  $\text{BaSiP}_3\text{N}_7$  the orientation of tetrahedra vertices alternates.

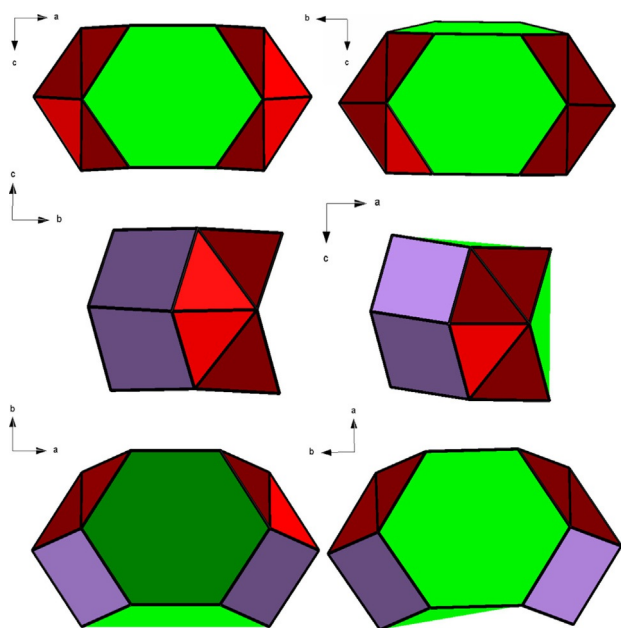


**Figure 2.** Tetrahedra connection patterns of  $\text{SrSiP}_3\text{N}_7$  (left) and  $\text{BaSiP}_3\text{N}_7$  (right). Patterns of both compounds show *dreier* (red), *vierer* (lilac), and *sechser* rings (green).

In the case of  $\text{BaSiP}_3\text{N}_7$ , the ordering of tetrahedra was considered by symmetry reduction and refinement of the structure against SCXRD data in subgroups  $Pna2_1$ ,  $P2_1ma$ , and  $P2_1/c$  of space group  $Pnma$ . Only subgroups retaining the extinction condition of the  $a$  glide planes present in  $Pnma$  were taken into account because electron diffraction parallel to  $[001]$  showed no violation of the extinction conditions. Additional electron diffraction patterns parallel to  $[100]$  showed no violation of the extinction conditions of the  $n$  glide, too, further supporting the structure model in space group  $Pnma$  (a comparison of experimental diffraction patterns with simulated ones based on the structure model in space group  $Pnma$  is given in Figure S5).

The comparison of resulting tetrahedral volumes showed the same features as for  $\text{SrSiP}_3\text{N}_7$  (Table S12). BVS calculations performed for the different structure models again suggested two sites completely occupied by P and two sites shared by Si and P (Tables S16–18). The simple approach of comparing tetrahedra volume as a tool for assigning Si and P, which lack scattering contrast, to the respective sites was indeed confirmed by scanning transmission electron microscope energy-dispersive X-ray spectroscopy (STEM-EDX) mapping with atomic resolution for  $\text{BaSiP}_3\text{N}_7$ . These data support the model in space group  $Pnma$ , showing two sites with mixed Si/P occupation (Figure 3, enlarged version see Figure S6). This result is also corroborated by  $^{31}\text{P}$  solid-state magic angle spinning (MAS)-NMR spectra, which show a broad signal [full width at half-maximum (fwhm) = 19.7 ppm] that is consistent with a dis-

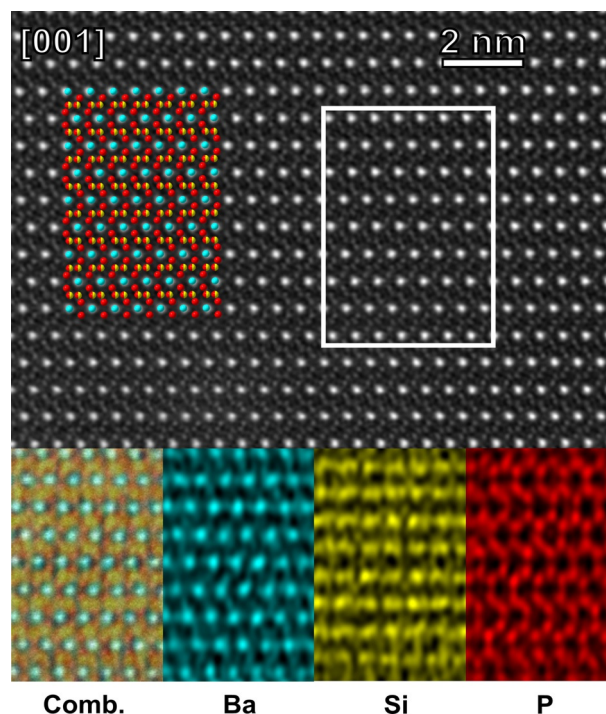


**Figure 3.** Atomic-resolution STEM-EDX of  $\text{BaSiP}_3\text{N}_7$  along  $[001]$ . STEM high-angle annular dark-field (HAADF) image (top) with structure overlay (Ba: cyan, P: red, Si: yellow). The inset shows the corresponding area for EDX maps (bottom) with a combined color map, Ba map (cyan), Si map (yellow), and P map (red).

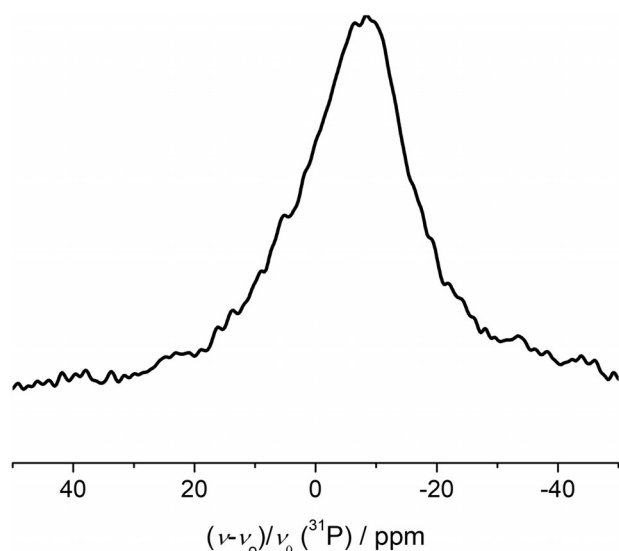


**Figure 4.**  $^{31}\text{P}$  NMR spectrum showing one broad signal for  $\text{BaSiP}_3\text{N}_7$  instead of two signals for the different crystallographic sites, most likely due to the occupational disorder.

ordered model (Figure 4, Figure S4). Line broadening in the NMR spectrum is probably due to disorder in the second coordination sphere of P atoms. In contrast, ordered nitrides like  $\text{BP}_3\text{N}_6$  or  $\text{Li}_{12}\text{P}_3\text{N}_9$  show very narrow signals in their  $^{31}\text{P}$  NMR spectra.<sup>[8,30]</sup>

In both structures, the connectivity of the tetrahedra via their vertices can explain the presence of different tetrahedral volumes. The smaller tetrahedra have three vertices occupied by twofold bridging nitrogen atoms  $\text{N}^{[2]}$  and one vertex occupied by a threefold bridging nitrogen atom  $\text{N}^{[3]}$ . The larger tetrahedra, in contrast, feature two vertices occupied by  $\text{N}^{[2]}$  and two vertices occupied by  $\text{N}^{[3]}$ . Chemical analysis by EDX agrees with the sum formulas. Due to ambiguous O contents (as indicated by EDX measurements) either surface hydrolysis or slight compositional variations cannot completely be ruled out so that a phase with according to  $\text{AESi}_{1+x}\text{P}_{3-x}\text{N}_{7-x}\text{O}_x$  ( $\text{AE}=\text{Sr}, \text{Ba}$ ) with  $x < 1$  could also be considered (Table S8) even though some analyses show no O.

Upon doping with  $\text{Eu}^{2+}$ , both compounds emit blue light under UV excitation. Luminescence spectra show emission maxima of  $\lambda_{\text{max}}=430$  nm for  $\text{SrSiP}_3\text{N}_7:\text{Eu}^{2+}$  and  $\lambda_{\text{max}}=424$  nm for  $\text{BaSiP}_3\text{N}_7:\text{Eu}^{2+}$  upon excitation with  $\lambda_{\text{exc}}=400$  nm. The emission curves were extrapolated to give an estimate of the fwhm, which amount to 45 nm ( $2404\text{ cm}^{-1}$ ) for  $\text{SrSiP}_3\text{N}_7:\text{Eu}^{2+}$  and 53 nm ( $2731\text{ cm}^{-1}$ ) for  $\text{BaSiP}_3\text{N}_7:\text{Eu}^{2+}$  (Figure 5). The corresponding Stokes shifts are 38 nm ( $2254\text{ cm}^{-1}$ ) for  $\text{SrSiP}_3\text{N}_7:\text{Eu}^{2+}$  and 32 nm ( $1925\text{ cm}^{-1}$ ) for  $\text{BaSiP}_3\text{N}_7:\text{Eu}^{2+}$ . The presence of a single narrow emission band for both phosphors can be explained by the emission properties of  $\text{Eu}^{2+}$  and the presence of a single crystallographic site for the alkaline earth ions suitable for doping with  $\text{Eu}^{2+}$  with  $\text{AE}-\text{N}$  distances ranging from 2.696(3)–3.270(3) Å ( $\text{SrSiP}_3\text{N}_7$ ) to 2.872(3)–3.230(3) Å ( $\text{BaSiP}_3\text{N}_7$ ). The similarity of emission properties in terms of fwhm are most likely to be explained by the  $\text{P}-\text{Si}_{0.5}\text{P}_{0.5}$  „cages“ around the AE position, which are very similar. Thus, only minute devia-

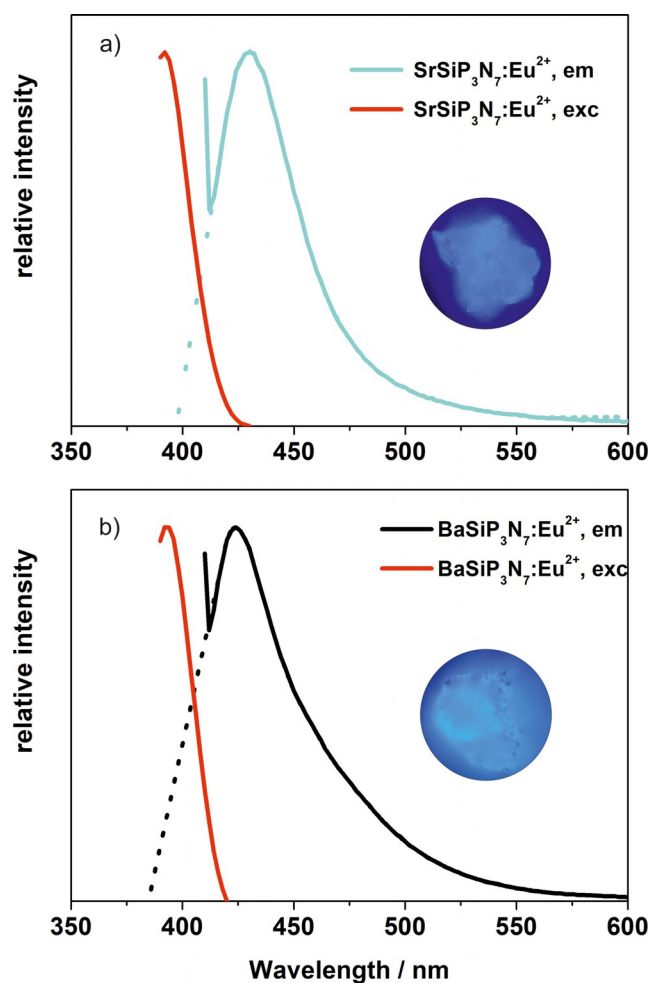


**Figure 5.** Emission spectra of (a)  $\text{SrSiP}_3\text{N}_7:\text{Eu}^{2+}$  (blue) and (b)  $\text{BaSiP}_3\text{N}_7:\text{Eu}^{2+}$  (black); measured data in solid lines and extrapolation in dotted lines; respective excitation spectra (red) (insets: micrographs of luminescent particles).

tions are caused by different AE cation sizes even though both structures differ with respect to their space groups, unit cell volumes, and tetrahedra orientations.

## Conclusions

High-pressure high-temperature synthesis with the addition of  $\text{NH}_4\text{F}$  is a suitable approach to the synthesis of mixed nitridosilicatephosphates. The compounds  $\text{AESiP}_3\text{N}_7$  ( $\text{AE}=\text{Sr}, \text{Ba}$ ) adopt the structure types of the two polymorphs of the mineral barylite. This structure type has not been observed for nitride compounds so far. Although silicon and phosphorus exhibit little contrast in X-ray diffraction, the comparison of polyhedra volumes led to structure models with an occupationally disordered site that also persists if potential ordering is considered by symmetry reduction. The disordered model for  $\text{BaSiP}_3\text{N}_7$  is further supported by solid-state NMR spectroscopy. Scanning transmission electron microscopy energy-dispersive X-ray spectroscopy (STEM-EDX) mapping with atomic resolution enables to directly observe said disorder, which is additionally in accordance with systematic absences observed in electron dif-

fraction patterns. Therefore, nitridosilicatephosphates have the potential to significantly diversify the structural chemistry of nitrides. Their suitability as host lattices for rare-earth activator ions seems especially intriguing considering the emission properties of other compounds with multiple tetrahedra centers like  $\text{CaAlSiN}_3:\text{Eu}^{2+}$ ,  $\text{Sr}[\text{Li}_2\text{Al}_2\text{O}_2\text{N}_2]:\text{Eu}^{2+}$ , or  $\text{Sr}[\text{LiAl}_3\text{N}_4]:\text{Eu}^{2+}$ .<sup>[2,31,32]</sup>

## Acknowledgements

Financial support by the Deutsche Forschungsgemeinschaft DFG (projects SCHN 377/18-1 and OE 513/6-1) is gratefully acknowledged. We thank Dr. Peter Mayer for single-crystal data collection, Dr. Thomas Bräuniger, Christian Minke, and Dr. Otto Zeman for NMR measurements, Lisa Gamperl (all at Department of Chemistry at LMU Munich) for SEM investigations and Dr. Philipp Strobel (Lumileds Phosphor Center Aachen) for luminescence measurements and helpful discussions. Open access funding enabled and organized by Projekt DEAL.

## Conflict of interest

The authors declare no conflict of interest.

**Keywords:** disordered compounds · high-pressure chemistry · nitrides · phosphorus · silicon

- [1] M. Zeuner, S. Pagano, W. Schnick, *Angew. Chem. Int. Ed.* **2011**, *50*, 7754–7775; *Angew. Chem.* **2011**, *123*, 7898–7920.
- [2] P. Pust, P. J. Schmidt, W. Schnick, *Nat. Mater.* **2015**, *14*, 454–458.
- [3] K. Uheda, N. Hirosaki, Y. Yamamoto, A. Naito, T. Nakajima, H. Yamamoto, *Electrochem. Solid-State Lett.* **2006**, *9*, H22.
- [4] L. Wang, R. J. Xie, T. Suehiro, T. Takeda, N. Hirosaki, *Chem. Rev.* **2018**, *118*, 1951–2009.
- [5] Y. Q. Li, A. C. A. Delsing, G. De With, H. T. Hintzen, *Chem. Mater.* **2005**, *17*, 3242–3248.
- [6] F. Wang, W. Wang, L. Zhang, J. Zheng, Y. Jin, J. Zhang, *RSC Adv.* **2017**, *7*, 27422–27430.
- [7] H. P. Baldus, W. Schnick, J. Lücke, U. Wannagat, G. Bogedain, *Chem. Mater.* **1993**, *5*, 845–850.
- [8] S. Vogel, A. T. Buda, W. Schnick, *Angew. Chem. Int. Ed.* **2018**, *57*, 13202–13205; *Angew. Chem.* **2018**, *130*, 13386–13389.
- [9] S. Wendl, L. Eisenburger, P. Strobel, D. Günther, J. P. Wright, P. J. Schmidt, O. Oeckler, W. Schnick, *Chem. Eur. J.* **2020**, *26*, 7292–7298.
- [10] S. D. Kloß, W. Schnick, *Angew. Chem. Int. Ed.* **2019**, *58*, 7933–7944; *Angew. Chem.* **2019**, *131*, 8015–8027.
- [11] A. Marchuk, F. J. Pucher, F. W. Karau, W. Schnick, *Angew. Chem. Int. Ed.* **2014**, *53*, 2469–2472; *Angew. Chem.* **2014**, *126*, 2501–2504.
- [12] D. Baumann, W. Schnick, *Inorg. Chem.* **2014**, *53*, 7977–7982.
- [13] D. Martin Knotter, T. J. J. (Dee) Denteneer, *J. Electrochem. Soc.* **2001**, *148*, F43.
- [14] H. Huppertz, *Z. Kristallogr. Cryst. Mater.* **2004**, *219*, 330–338.
- [15] S. Merlino, C. Biagioni, E. Bonaccorsi, N. V. Chukanov, I. V. Pekov, S. V. Krivovichev, V. N. Yakovenchuk, T. Armbruster, *Mineral. Mag.* **2015**, *79*, 145–155.
- [16] V. A. Blatov, A. P. Shevchenko, D. M. Proserpio, *Cryst. Growth Des.* **2014**, *14*, 3576–3586.
- [17] K. Momma, F. Izumi, *J. Appl. Crystallogr.* **2011**, *44*, 1272–1276.
- [18] T. Schlieper, W. Milius, W. Schnick, *Z. Anorg. Allg. Chem.* **1995**, *621*, 1380–1384.
- [19] H. Yamane, T. Nagura, T. Miyazaki, *Acta Crystallogr. Sect. E* **2014**, *70*, i23–i24.
- [20] C. Schmolke, D. Bichler, D. Johrendt, W. Schnick, *Solid State Sci.* **2009**, *11*, 389–394.
- [21] G. Pilet, H. A. Höpfe, W. Schnick, S. Esmaeilzadeh, *Solid State Sci.* **2005**, *7*, 391–396.
- [22] M. Woike, W. Jeitschko, *Inorg. Chem.* **1995**, *34*, 5105–5108.
- [23] J. David, Y. Laurent, J.-P. Charlot, J. Lang, *Bull. Soc. Fr. Mineral. Cristallogr.* **1973**, *96*, 21–24.
- [24] F. W. Karau, W. Schnick, *J. Solid State Chem.* **2005**, *178*, 135–141.
- [25] S. D. Kloß, N. Weidmann, R. Niklaus, W. Schnick, *Inorg. Chem.* **2016**, *55*, 9400–9409.
- [26] K. Landskron, W. Schnick, *J. Solid State Chem.* **2001**, *156*, 390–393.
- [27] R. Marchand, P. L'Haridon, Y. Laurent, *J. Solid State Chem.* **1982**, *43*, 126–130.
- [28] K. Landskron, E. Irran, W. Schnick, *Chem. Eur. J.* **1999**, *5*, 2548–2553.
- [29] N. E. Brese, M. O'Keeffe, *Acta Crystallogr. Sect. B* **1991**, *47*, 192–197.
- [30] E. Bertschler, R. Niklaus, W. Schnick, *Chem. Eur. J.* **2017**, *23*, 9592–9599.
- [31] X. Piao, K. I. Machida, T. Horikawa, H. Hanzawa, Y. Shimomura, N. Kijima, *Chem. Mater.* **2007**, *19*, 4592–4599.
- [32] G. J. Hoerder, M. Seibald, D. Baumann, T. Schröder, S. Peschke, P. C. Schmid, T. Tyborski, P. Pust, I. Stoll, M. Bergler, C. Patzig, S. Reißaus, M. Krause, L. Berthold, T. Höche, D. Johrendt, H. Huppertz, *Nat. Commun.* **2019**, *10*, 1824.

Manuscript received: December 28, 2020

Revised manuscript received: January 18, 2021

Accepted manuscript online: January 19, 2021

Version of record online: February 4, 2021